

**Transition state structure and inhibition of Rv0091,  
a 5'-deoxyadenosine / 5'-methylthioadenosine nucleosidase from  
*Mycobacterium tuberculosis***

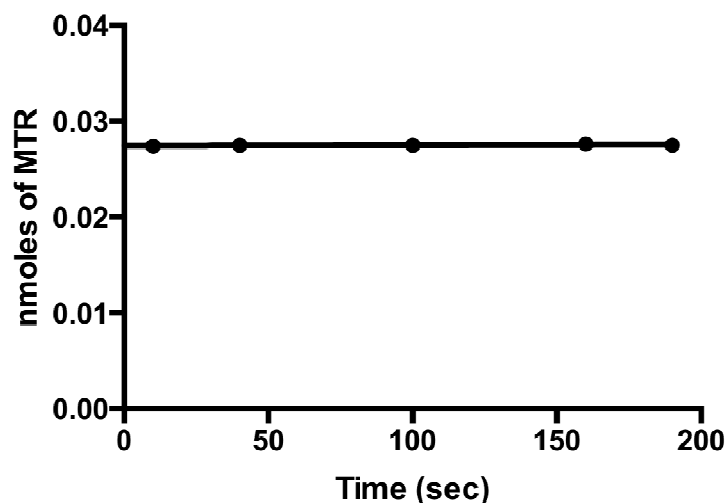
Hilda A. Namanja-Magliano<sup>†</sup>, Christopher F. Stratton,<sup>†</sup> & Vern L. Schramm\*

Department of Biochemistry, Albert Einstein College of Medicine, 1300 Morris Park Avenue,  
Bronx, New York 10461, United States

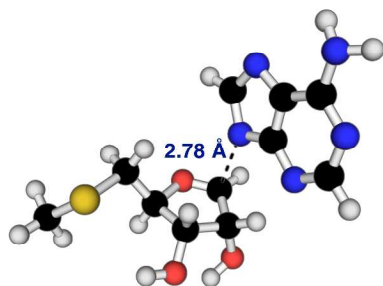
<sup>†</sup>These authors contributed equally to this work.

**Supporting Information**

<b>A. Supporting Information Figure S1–S5</b>	<b>S2</b>
<b>B. Supporting Information Tables S1–S2</b>	<b>S5</b>
<b>C. Methods</b>	<b>S6</b>
<i>Expression and purification of Rv0091</i>	S6
<i>Kinetic assays of Rv0091</i>	S6
<i>Oligomeric state determination</i>	S6
<i>Synthesis of isotopically labeled MTA substrates</i>	S7
<i>Measurement of KIEs and forward commitment</i>	S8
<i>Computational analysis</i>	S9
<i>Determination of inhibition constants</i>	S15
<b>D. Supporting Information References</b>	<b>S16</b>

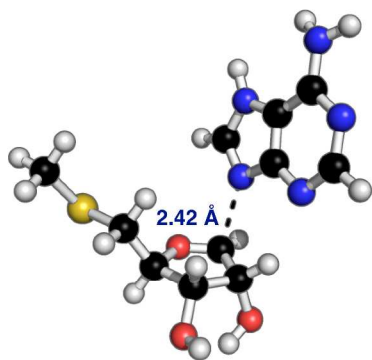
**A. SUPPORTING INFORMATION FIGURES S1–S5**

**Figure S1. Measurement of forward commitment ( $C_f$ ) for the MTA hydrolysis with Rv0091.** Rv0091 was mixed with [5'- $^{14}\text{C}$ ]-MTA and incubated for 40 sec to form 0.0274 nmol MTR (time 0 on the abscissa). At that time the reaction was chased with a large excess of unlabeled MTA and the synthesis of additional MTR after the chase was monitored to 180 sec. After extrapolation to the origin [MTR] =  $0.0274 \pm 0.0001$  nmoles; using eq. 8 and 9 the  $C_f$  determined was  $0.0794 \pm 0.0002$ . MTA, 5'-methylthioadenosine; MTR, 5'-methylthioribose. Data was plotted using GraphPad Prism 6.



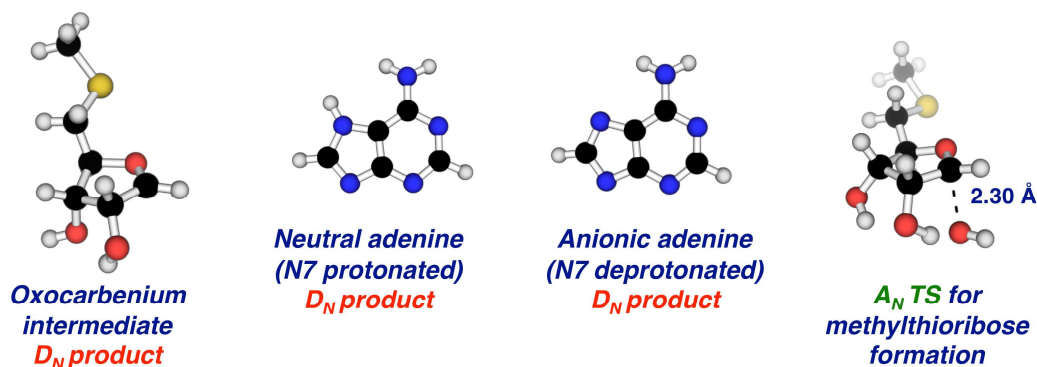
	Intrinsic KIEs	Calculated KIEs
1'- $^{14}\text{C}$	$1.038 \pm 0.005$	1.038
1'- $^3\text{H}$	$1.207 \pm 0.009$	1.347
9- $^{15}\text{N}$	$1.021 \pm 0.007$	1.030
7- $^{15}\text{N}$	$0.998 \pm 0.005$	1.006
5'- $^3\text{H}$	$0.998 \pm 0.008$	0.942

**Figure S2. Model for the Rv0091 TS structure ( $\text{D}_\text{N}^\ddagger\text{A}_\text{N}$ ) with anionic leaving (N7 deprotonated) group and calculated KIE values.** The TS structure was optimized (Gaussian 09, RB3LYP/ 6-31g(d) theory)<sup>1</sup> with the C1'–N9 bond length fixed at 2.78 Å; no additional constraints were applied to the structure. Predicted KIEs were calculated (ISOEFF98)<sup>2</sup> from the scaled vibrational frequencies of optimized structures for MTA and the TS structure.



	Intrinsic KIEs	Calculated KIEs
1'- <sup>14</sup> C	1.038 ± 0.005	1.038
1'- <sup>3</sup> H	1.207 ± 0.009	1.239
9- <sup>15</sup> N	1.021 ± 0.007	1.024
7- <sup>15</sup> N	0.998 ± 0.005	0.986
5'- <sup>3</sup> H	0.998 ± 0.008	0.990

**Figure S3. Model for the Rv0091 TS structure ( $D_N^{\ddagger}A_N$ ) with neutral leaving group (N7 protonated) and calculated KIE values.** The TS structure was optimized (Gaussian 09, RB3LYP/ 6-31g(d) theory)<sup>1</sup> with the C1'-N9 bond length fixed at 2.42 Å; no additional constraints were applied to the structure. Predicted KIEs were calculated (ISOEFF98)<sup>2</sup> from the scaled vibrational frequencies of optimized structures for MTA and the TS structure.



	Intrinsic KIEs	Calculated EIEs ( $D_N$ )	Calculated KIEs ( $A_N^{\ddagger}$ )	EIE*KIE
1'- <sup>14</sup> C	1.038 ± 0.005	1.000	1.051	1.051
1'- <sup>3</sup> H	1.207 ± 0.009	1.349	0.920	1.241
<i>Neutral adenine (N7 protonated)</i>	9- <sup>15</sup> N 1.021 ± 0.007	1.024	-	-
	7- <sup>15</sup> N 0.998 ± 0.005	0.985	-	-
<i>Anionic adenine (N7 deprotonated)</i>	9- <sup>15</sup> N 1.021 ± 0.007	1.028	-	-
	7- <sup>15</sup> N 0.998 ± 0.005	1.004	-	-
5'- <sup>3</sup> H	0.998 ± 0.008	1.005	1.000	1.005

**Figure S4. Model for the Rv0091 TS structure ( $D_N^{\ddagger}A_N^{\ddagger}$ ) with neutral (N7 protonated) and anionic (N7 deprotonated) leaving groups.** EIEs for oxocarbenium formation were calculated (ISOEFF98)<sup>2</sup> from the scaled vibrational frequencies of optimized structures (Gaussian 09, RB3LYP/ 6-31g(d) theory)<sup>1</sup> of MTA, the oxocarbenium intermediate, neutral adenine (N7 protonated), and anionic adenine (N7 deprotonated). The TS structure for methylthioribose formation was optimized with the C1'-Ow bond distance fixed at 2.30 Å; no additional constraints were applied to the structure. KIEs were calculated from the scaled vibrational frequencies of optimized structures for the oxocarbenium intermediate and the TS structure.

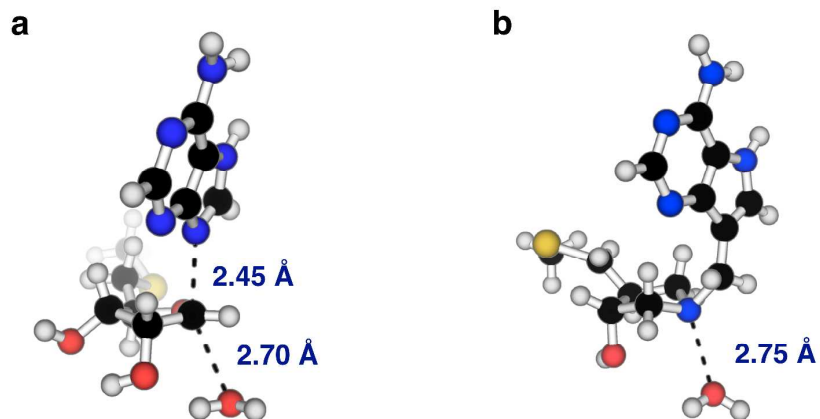


**Figure S5. Rv0091 TS structure and MT-DADMe-ImmA bound to *E. coli* MTAN.** (a) Calculated model for the TS structure of MTA hydrolysis by Rv0091. The best match to the intrinsic KIE values was found with the water molecule at a distance of 2.70 Å from the C1' reaction center. (b) Coordinates for the structure of MT-DADMe-ImmA bound to *E. coli* MTAN (PDB: 1Y6Q). The nucleophilic water is present in the crystal structure at distance of 2.75 Å from the 1' position of the ribose ring.

**B. SUPPORTING INFORMATION TABLES S1–S2**

Bond	Bond Length (Å)			Bond Order		
	Ground State	Transition State	$\Delta$ (TS–GS)	Ground State	Transition State	$\Delta$ (TS–GS)
C1'N9	1.466	2.450	+0.984	0.909	0.171	-0.738
C1'–H1'	1.094	1.080	-0.014	0.876	0.884	+0.0085
C1'–O4	1.418	1.273	-0.145	0.925	1.393	+0.468
C1'–Ow	NA	2.700	-	NA	0.074	-

**Table S1. Bond lengths and bond orders for the TS structure model of Rv0091.** Values correspond to the TS structure shown in Figure 4 of the main text. Ground state values refer to the optimized structure of MTA.

Atom	Ground State	Transition State	$\Delta$ (TS–GS)
C1'	0.270	0.452	+0.182
N9	-0.436	-0.543	-0.107
N7	-0.494	-0.547	-0.053
O4	-0.588	-0.410	+0.178

**Table S2. NBO calculations the ground state and TS models of Rv0091.** Values correspond to the TS structure shown in Figure 4 of the main text. Ground state values refer to the optimized structure of MTA.

## **C. METHODS**

**Expression and purification of Rv0091.** A synthetic gene was designed for Rv0091 (NCBI GenBank: CCP42816.1) and purchased from DNA2.0 Inc. in a pJexpress414 expression vector. The expression vector contained sequences to encode for an *N*-terminus His<sub>6</sub> tag and a thrombin cleavage site. Rv0091 was expressed in *E. coli* using the BL21 Star<sup>TM</sup> (DE3) plysS cell line. A 25 mL pre-culture in LB, ampicillin (100 µg/mL) and chloramphenicol (100 µg/mL) medium was incubated overnight at 37°C. The following day, 6 mL of pre-culture was added to 1 L of fresh LB-ampicillin (100 µg/mL) and incubated at 37°C to OD<sub>600</sub> = 0.6. The culture was induced with 0.5 mM isopropyl-D-thiogalactoside (IPTG) and incubated overnight at 28°C. Cells were harvested the next day via centrifugation and re-suspended in 20 mM Tris-HCl, 300 mM NaCl, 10 mM imidazole, pH = 7.4). Lysozyme and DNase were added to the cells and incubated at 4°C for 20 min. Cells were lysed via sonication and cell debris was removed by centrifugation. Ni-NTA resin (Qiagen) was employed for purification of the enzyme, which was eluted with a gradient of 30 mM to 250 mM imidazole in 20 mM Tris-HCl, 300 mM NaCl, pH = 7.4. Fractions containing Rv0091 were identified by SDS-PAGE and exchanged into 50 mM HEPES, pH = 7.4 and 10% glycerol by dialysis. The protein was concentrated and stored at –80°C.

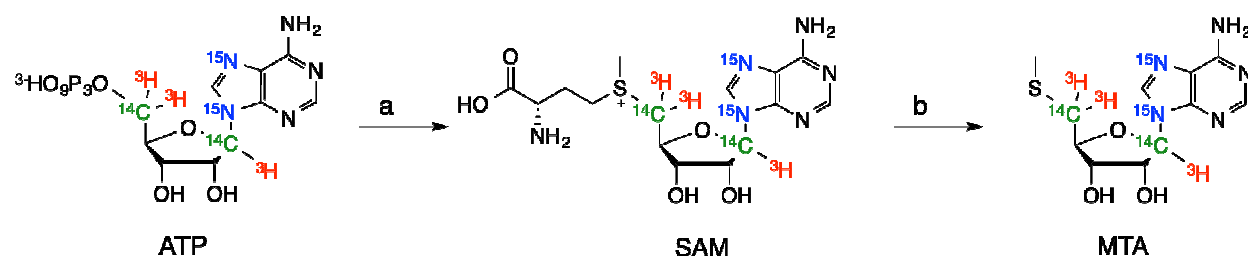
**Kinetic assays of Rv0091.** Steady-state kinetics were performed as previously described using a coupled luminescence assay that converts the product adenine to ATP, which is consequently detected by firefly luciferase.<sup>3</sup> Rv0091 (100 nM) was used and reactions were initiated by adding substrate (MTA, SAH, or 5'-dAdo) at varying concentrations (0.1 – 700 µM). The data was fitted using GraphPad Prism 6 and kinetic parameters were determined by fitting the data to the Michaelis-Menten eq. 3 where  $K_M$  represents the Michaelis–Menten constant for the substrate (A) and  $k_{cat}$  is the turnover number of Rv0091 (*e*).

$$v / e = (k_{cat} A) / (K_M + A) \quad (3)$$

**Oligomeric state determination.** Rv0091 oligomerization was characterized by cross-linking with glutaraldehyde as previously described with slight modifications.<sup>4</sup> Briefly, 0.8 mg/mL of protein in 50 mM phosphate, 50 mM NaCl, pH 7.5 was subjected to 0.1 – 2 % (v/v)

glutaraldehyde (Sigma-Aldrich) for 30 minutes. The reactions were stopped by addition of an equal volume of 500 mM Tris-Cl, pH 7.4 (Sigma-Aldrich) and analyzed by SDS-PAGE.

**Synthesis of isotopically labeled MTA substrates.** [9-<sup>15</sup>N] and [7-<sup>15</sup>N]-Adenine were synthesized as previously described.<sup>5</sup> [1'-<sup>3</sup>H], [1'-<sup>14</sup>C], [5'-<sup>3</sup>H<sub>2</sub>], [5'-<sup>14</sup>C] [9-<sup>15</sup>N / 5'-<sup>14</sup>C] and [7-<sup>15</sup>N / 5'-<sup>14</sup>C]-ATPs were prepared enzymatically from glucose or ribose as previously described.<sup>6</sup> [1'-<sup>3</sup>H], [1'-<sup>14</sup>C], [5'-<sup>3</sup>H<sub>2</sub>], [9-<sup>15</sup>N / 5'-<sup>14</sup>C] and [7-<sup>15</sup>N / 5'-<sup>14</sup>C] labeled MTAs were obtained from labeled-ATP substrates (**Scheme S1**).



**Scheme S1. Synthesis of isotopically labeled MTA substrates.** (a) Methionine, *hMAT2A*, pH 37 °C, 3.5 hrs (b) pH 4.0, 75 °C, 3.5 hrs

Human MAT2A (*hMAT2A*) was purified according to Shafqat and co-workers.<sup>7</sup> Labeled SAM was prepared using *hMAT2A* from the corresponding labeled ATP and methionine. A typical reaction contained 4 μM *hMAT2A*, 1.1 mM L-methionine, 0.8 – 1 mM of labeled ATP, 50 mM Tris – HCl pH 8.0, 50 mM KCl and 1 mM MgCl<sub>2</sub>. The reaction was allowed to go for 3.5 hrs at 37 °C and purified by RP-HPLC using a C18-luna analytical column, 250 X 4.6 mm, 5 μm (Phenomenex) with a solvent system containing water 50 mM ammonium formate pH 4.0 (buffer A) and 0.1% formic acid/acetonitrile (buffer B). SAM was purified at a gradient of 0 – 90 % buffer B over 20 minutes. The isolated SAMs were dried by centrifugation *in vacuo*. Labeled MTA substrates were synthesized from SAM by hydrolysis in sodium citrate buffer pH 4.0 at 75 °C for 3.5 hours as described elsewhere.<sup>8</sup>

**Measurement of KIEs and forward commitment.** V/K KIEs were measured using the competitive approach by comparing products formed from isotopically labeled substrate pairs as

previously described.<sup>8</sup> MTR products were eluted on charcoal-cellulose columns with 50 mM ribose, 50 mM potassium phosphate (pH 6.0). Fractions (2 mL) were collected, dried and radioactivity was counted for 10 min. Scintillation counting was performed in dual fashion on a Tri-carb 2910TR scintillation counter (Perkin-Elmer). <sup>3</sup>H appears in Channel A and <sup>14</sup>C appears in both Channel A and Channel B. Therefore, the total counts for <sup>3</sup>H and <sup>14</sup>C, were deconvoluted using control [5'-<sup>14</sup>C] or [1'-<sup>14</sup>C] MTR to determine relative amounts of <sup>14</sup>C ratio (*r*) between Channel A and Channel B (eq. 4). Total <sup>3</sup>H and <sup>14</sup>C were calculated from eq. 5 and eq. 6 respectively.

$$r = \text{Channel A} / \text{Channel B} \quad (4)$$

$$^3\text{H} = \text{Channel A} - (\text{Channel B} \times r) \quad (5)$$

$$^{14}\text{C} = \text{Channel B} + (\text{Channel B} \times r) \quad (6)$$

The KIEs were corrected to 0% hydrolysis of the substrate and calculated by the eq. 7, where *f* is the fraction of reaction conversion. R is the ratio of heavy to light isotope at partial (*R<sub>f</sub>*) and completion (*R<sub>0</sub>*) of the reaction, respectively.

$$\text{KIE}_{VK} = \ln(1 - f) / \ln(1 - f (R_f / R_0)) \quad (7)$$

The forward commitment *C<sub>f</sub>* (**Figure S1**) to catalysis was measured by the isotope trapping method.<sup>9</sup> The pulse mixture (50 mM HEPES pH 7.4, 1 mM DTT and 100 μM of [5'-<sup>14</sup>C] MTA) was mixed enzyme to give a reaction mixture of 40 μL (10 μM Rv0091) at 25 °C. After 40 sec (less than one catalytic turnover), the reaction was chased with 660 μL of 50 mM HEPES pH 7.4, 1 mM DTT and 8 mM unlabeled MTA. Samples (100 μL) were quenched at different times ranging from 10 to 160 sec and quantified for product formation (MTR) by elution on charcoal-cellulose columns and counting as described above. Commitment was calculated from the amount of labeled MTR product formed after addition of chase solution and the data was fitted to a least-squares fit (GraphPad Prism 6). The equation of the fitted curve was used to calculate product formed (*P*) at time zero. *C<sub>f</sub>* was determined from eq. 8 where *Y* is the ratio of moles of MTR product (*P*) to moles of Rv0091-MTA (*ES*) complex. *ES* is calculated from eq. 9, where *E*



is total enzyme used, S is the total MTA substrate in the pulse and  $K_M$  is the Michaelis constant for MTA.

$$C_f = Y / (1 - Y) \quad (8)$$

$$ES = (ES) / (S + K_M) \quad (9)$$

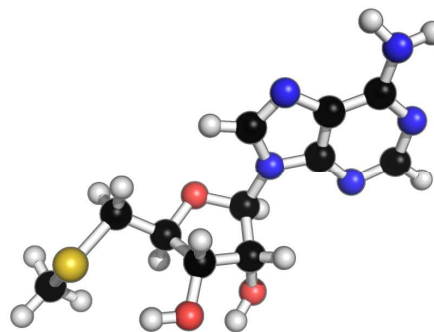
**Computation analysis.** The Rv0091 TS structure was modeled via density functional theory calculations using the B3LYP functional and 6-31g(d) basis set as implemented in Gaussian 09.<sup>1</sup> KIEs were calculated using ISOEFF98<sup>2</sup> from the scaled vibrational frequencies of optimized structures for MTA in the GS and each TS structure, as detailed below. All TS structures displayed a single calculated imaginary frequency corresponding to atomic motion along the reaction coordinate.

The optimized structure for MTA in the GS was calculated using water as an implicit solvent model (PCM) and was identical for all KIE calculations. The input coordinates for the optimization of MTA were taken from the PubChem 3D database (CID: 439176).<sup>10</sup> The optimized MTA GS structure was located as global minimum and displayed no imaginary frequencies. The input geometry for TS structure searches were taken from the coordinates for the binary complex of 5'-methylthiotubercidin bound to *E. coli* MTAN (PDB: 1NC1).<sup>11</sup> For the TS structures reported in **Figure S2** and **Figure S3**, optimized structures were generated using water as implicit solvent model with the C1'-N9 bond fixed at 1.6, 1.8, 2.0, 2.2, 2.4, 2.6, 2.8, or 3.0 Å. No additional constraints were applied to the structures. TS structures were refined through optimizing structures with the C1'-N9 bond at fixed distances varied by 0.01 Å. For the TS structure reported in **Figure S4**, equilibrium EIEs were calculated using the MTA GS and optimized structures for the oxocarbenium intermediate, and adenine in the neutral (N7 protonated) and anionic (N7 deprotonated) forms. KIEs were calculated for nucleophilic attack of water on the oxocarbenium intermediate using TS structures optimized with the C1'-Ow bond length fixed at 1.7, 1.9, 2.1, 2.3, 2.3, 2.5, and 2.7 Å. No additional constraints were applied to the structures. The final TS structure for Rv0091 reported in Figure 4 of the main text was located by optimizing structures with a C1'-N9 bond length fixed at 2.43, 2.44, and 2.45 Å and the C1'-Ow bond length fixed at 2.65, 2.70, or 2.75 Å. NBO analysis and single point energy calculations

were performed on the optimized structures using the NBO3.0 program available in Gaussian 09. EPS maps were visualized in GaussView 5.0 (isovalue = 0.04) from the electron density and potential cubes acquired from the checkpoint files of single point energy calculations. Bond orders were calculated based on Wiberg's formula.<sup>1</sup>

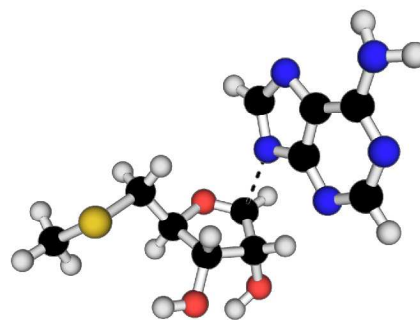
### Atomic coordinates for the optimized MTA ground state structure:

C	-0.60017600	1.44263800	-0.40443100
C	-0.03679600	0.60909700	0.76552400
O	-1.06860600	-0.26164000	1.20042400
C	-2.28313800	0.00117800	0.46458200
C	-1.79268800	0.59231600	-0.86950600
N	1.12561300	-0.20348700	0.39609700
C	2.42019700	0.25990400	0.28412200
C	3.17977700	-0.85742600	-0.07825800
N	2.38438300	-1.98586600	-0.18343800
C	1.17735100	-1.55270200	0.10575700
C	4.56370400	-0.63642000	-0.25184000
N	5.04845500	0.60770500	-0.05678200
C	4.19171000	1.58266700	0.28880300
N	2.87047600	1.50937700	0.47975600
N	5.41658800	-1.61567700	-0.64235500
C	-3.07867600	-1.29462200	-0.36620800
S	-4.66967300	-1.07673700	-0.53212900
C	-5.71795300	-0.32817800	0.76987300
O	-2.72452400	1.43309100	-1.52419300
O	-1.06292400	2.67507300	0.12168700
H	4.63898300	2.56442500	0.43322300
H	0.28742400	-2.16258400	0.14475700
H	0.27875800	1.27598800	1.57384500
H	0.14940700	1.60085000	-1.18937700
H	-1.44784000	-0.21504200	-1.53156200
H	-2.86220200	0.76854800	0.99414400
H	-1.85596300	2.89741100	-0.40256400
H	-2.51519700	-2.04317900	-0.19954400
H	-3.28250700	-1.70409100	1.36011400
H	-6.70916600	-0.19323600	0.33049200
H	-5.79414600	-1.00073500	1.62795700
H	-5.33523000	0.64385400	1.08795700
H	-3.56997700	0.94466600	-1.56895300
H	5.11453800	-2.57763900	-0.57641600
H	6.40786300	-1.43870000	-0.55129600



**Atomic coordinates for the Rv0091 TS structure ( $D_N^{\ddagger}A_N$ ) shown in Figure S2 with adenine as an anionic leaving group:**

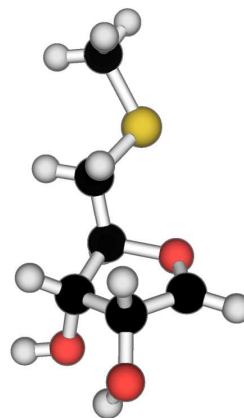
C	-0.96166500	2.03085900	0.26364400
C	-1.02596500	1.48691700	1.66229800
O	-1.91750100	0.60940400	1.85692000
C	-2.53461100	0.17323000	0.54776900
C	-1.72264600	0.93858600	-0.52597500
N	1.11946100	-0.15786100	1.01403000
C	2.13086700	0.18317100	0.16336000
C	3.17578000	-0.75622700	0.32393400
N	2.82659800	-1.68528600	1.28231500
C	1.60854600	-1.26223700	1.64310800
C	4.32289400	-0.57843900	-0.46866600
N	4.37845400	0.45968100	-1.32603800
C	3.31190600	1.28397800	-1.38614500
N	2.17220000	1.22946000	-0.70091300
N	5.38134900	-1.45688000	-0.44079400
C	-2.46438200	-1.34069400	0.48113600
S	-3.24535600	-1.92415000	-1.07530700
C	-5.01737500	-1.90193600	-0.61109500
O	-2.54533800	1.58769200	-1.47143300
O	-1.70033300	3.24526900	0.35602000
H	3.40721100	2.10706400	-2.09460700
H	1.02512300	-1.77375500	2.40304700
H	-0.52227000	1.88615100	2.53747500
H	0.05729800	2.19456200	-0.09466500
H	-1.00012000	0.26943000	-1.00155800
H	-3.55928500	0.54316900	0.61058500
H	-2.46201900	3.14733200	-0.24983600
H	-1.41979500	-1.66351700	0.45633600
H	-2.95634800	-1.80340200	1.34036300
H	-5.56437300	-2.26711100	-1.48353000
H	-5.19910100	-2.57100200	0.23337700
H	-5.36395800	-0.89356000	-0.37475700
H	-3.02565800	0.90600000	-1.97396200
H	5.47229400	-2.01024400	0.40186900
H	6.25554100	-1.09068700	-0.79769800



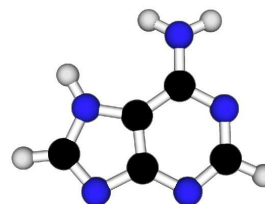


**Atomic coordinates for the structure of the oxocarbenium intermediate used in calculating the EIE for the  $D_N^*A_N^\ddagger$  mechanism in Figure S4:**

C	-2.01654400	-0.43726000	0.72391300
C	-1.38751000	-1.43547100	-0.20974300
O	-0.36209000	-1.02844900	-0.80436200
C	-0.05792600	0.43823200	-0.43721100
C	-1.37544200	0.89256400	0.21801700
C	1.18458700	0.46778900	0.42770900
S	2.61667400	-0.30287600	-0.42861500
C	3.95034400	0.25183900	0.69225000
O	-2.27037500	1.40198000	-0.74865100
O	-3.40580600	-0.45590500	0.72592000
H	-1.72279000	-2.45211800	-0.41080500
H	-1.64811200	-0.68691800	1.73063500
H	-1.19837900	1.59182000	1.03705500
H	0.09921000	0.89738900	-1.41243900
H	-3.67673700	0.15851100	0.01298500
H	1.40563600	1.52496000	0.61123200
H	1.01183200	-0.01559400	1.39479500
H	4.88052800	-0.15517200	0.28911000
H	4.01388800	1.34277300	0.71216100
H	3.79870900	-0.13600500	1.70253400
H	-2.30946000	2.36919600	-0.68229200

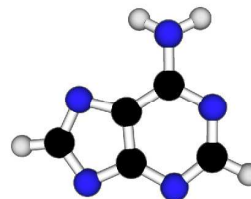
**Atomic coordinates for the structure of adenine (N7 protonated) used in calculating the EIE for the  $D_N^*A_N^\ddagger$  mechanism in Figure S4:**

N	-2.11581200	0.74816800	0.00977700
C	-0.73595500	0.81043600	0.00592600
C	-0.18624800	-0.48437500	-0.00503500
N	-1.27455000	-1.33735100	-0.00936200
C	-2.38388500	-0.54311200	-0.00080700
C	1.21434000	-0.62518800	-0.00324800
N	1.95206800	0.49830200	-0.00391700
C	1.31752900	1.68644900	-0.00272100
N	0.01098200	1.93541500	0.00699000
N	1.86653100	-1.82461800	-0.05558800
H	1.97353500	2.55559300	-0.00404900
H	-3.37694800	-0.97270200	-0.00386200
H	1.39527700	-2.65346200	0.28117700
H	2.85534800	-1.78591600	0.15952900
H	-1.27643400	-2.34818300	-0.03278300

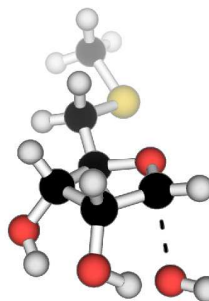


**Atomic coordinates for the structure of adenine (N7 deprotonated) used in calculating the EIE for the  $D_N^*A_N^\ddagger$  mechanism in Figure S4:**

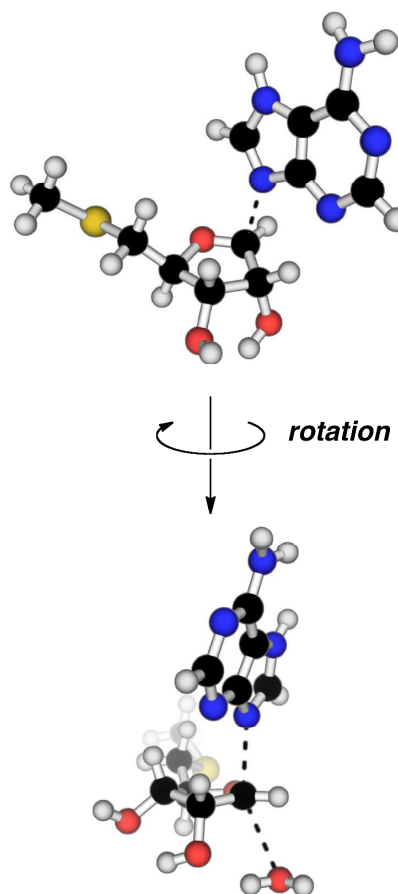
N	-2.14410100	0.67835000	0.00836500
C	-0.78407200	0.78659100	-0.00126200
C	-0.21729400	-0.51588200	-0.01142600
N	-1.22312100	-1.45632800	-0.00739800
C	-2.31492700	-0.66904400	0.00497300
C	1.18258100	-0.61127200	-0.01046500
N	1.92529400	0.51190800	0.00054300
C	1.26703400	1.69332400	0.00370900
N	-0.04153300	1.92810100	0.00333800
N	1.84056500	-1.82696200	-0.07295700
H	1.91303900	2.57279000	0.01112500
H	-3.31374800	-1.10101800	0.01151700
H	1.30673900	-2.61569500	0.27197800
H	2.79431400	-1.80385700	0.26897700

**Atomic coordinates for the  $A_N$  TS structure used in calculating the KIEs for the  $D_N^*A_N^\ddagger$  mechanism in Figure S4:**

C	-2.06916900	0.32225500	0.86629300
C	-1.42100800	-1.05033800	0.84414300
O	-0.17864000	-1.04600300	0.51055500
C	0.17602100	0.23529100	-0.17290300
C	-0.93042600	1.22879800	0.24641300
C	1.58623300	0.61601700	0.22251200
S	2.81716900	-0.63900300	-0.31772400
C	4.35297500	0.26569700	0.08957300
O	-1.43680900	1.94908800	-0.84674500
O	-3.24862700	0.39860700	0.13693400
H	-2.24313900	0.58880100	1.91876900
H	-0.54074700	1.91998600	1.00302500
H	0.09186600	0.01297800	-1.23929900
H	-3.15178700	-0.47799800	-0.51272500
H	1.81493000	1.56954800	-0.26583700
H	1.64970300	0.76105700	1.30617900
H	5.18493200	-0.38687500	-0.18576300
H	4.42287400	1.19545800	-0.48142900
H	4.40751300	0.48058000	1.16009300
H	-2.37005900	1.62980900	-0.90927000
H	-1.76112000	-1.92702100	1.38452800
O	-2.59361400	-1.61368400	-1.05260000
H	-3.08591400	-2.35265200	-0.65602400

**Atomic coordinates for the Rv0091 TS structure shown in Figure 4 of the main text:**

C	0.75498100	-1.97526800	-0.27544700
C	0.94905900	-1.19043600	1.00523400
O	1.87817300	-0.32216100	-0.94490700
C	2.44383800	-0.21245400	-0.43588300
C	1.48006300	-1.04725300	-1.30107200
N	-1.04327800	0.18587700	0.63260100
C	-2.27129000	-0.13325600	-0.08575300
C	-3.18264300	0.89834100	0.35201700
N	-2.46920700	1.84165300	1.07367000
C	-1.20915700	1.36434300	1.21137100
C	-4.50439200	0.76251400	-0.12365800
N	-4.79903800	-0.35245800	-0.81713000
C	-3.83757700	-1.26962100	-1.01676400
N	-2.57031200	-1.24810200	-0.60682600
N	-5.47708700	1.69656800	0.03172200
C	2.56181600	1.24845800	-0.81077000
S	3.75994700	2.13752000	0.26202700
C	3.84349800	3.71858800	-0.65280500
O	2.25429900	-1.80279900	-1.12886000
O	1.45586600	-3.20571900	-0.15609100
H	-4.14417900	-2.14493300	-1.58581800
H	-0.44231600	1.91079700	1.74245100
H	0.51692700	-1.38732400	1.97484700
H	-0.30238000	-2.13885600	-0.49558000
H	0.75506800	-0.40871800	-1.81087100
H	3.41948800	-0.69975500	-0.37471100
H	2.04360700	-3.24145600	-0.94345900
H	2.91728200	1.27887100	-1.84681100
H	1.58086700	1.73223500	-0.76878600
H	4.53561700	4.36065400	-0.10298500
H	4.22484700	3.56396900	-1.66555300
H	2.86313500	4.20041000	-0.69065500
H	1.71943000	-1.98912500	-3.00269800
H	-5.40602700	2.39564500	0.75769200
H	-6.41663900	1.40557400	-0.20672900
O	2.30911700	-3.00473400	2.47103200
H	1.70530600	-3.53468500	3.01589400
H	2.22795100	-3.40085800	1.58130400
H	-2.79348200	2.73203800	1.42822800



**Determination of inhibition constants.**  $K_i$  was determined as previously described.<sup>3</sup> Briefly, Rv0091 activity was measured with varying concentrations of inhibitor in the presence of 1 mM MTA and 1.0 unit of xanthine oxidase (Sigma-Aldrich) and then monitored at 305 nm. The reactions were initiated by adding 10 nM of enzyme. The  $K_i$  values were obtained from the rates with and without inhibitors ( $v_i / v_0$ ) that was fitted using the Morrison equation of tight-binding inhibitors on GraphPad Prism 6.<sup>12</sup>

## **D. SUPPORTING INFORMATION REFERENCES**

1. Frisch, M. J. T., G. W.; Schlegel, H. B.; Scuseria, G. E.; Robb, M. A.; Cheeseman, J. R.; Scalmani, G.; Barone, V.; Mennucci, B.; Petersson, G. A.; Nakatsuji, H.; Caricato, M.; Li, X.; Hratchian, H. P.; Izmaylov, A. F.; Bloino, J.; Zheng, G.; Sonnenberg, J. L.; Hada, M.; Ehara, M.; Toyota, K.; Fukuda, R.; Hasegawa, J.; Ishida, M.; Nakajima, T. E.; Honda, Y.; Kitao, O.; Nakai, H.; Vreven, T.; Montgomery, J. A.; Peralta, J. E.; Ogliaro, F.; Bearpark, M.; Heyd, J. J.; Brothers, E.; Kudin, K. N.; Staroverov, V. N.; Kobayashi, R.; Normand, J.; Raghavachari, K.; Rendell, A.; Burant, J. C.; Iyengar, S. S.; Tomasi, J.; Cossi, M.; Rega, N.; Millam, J. M.; Klene, M.; Knox, J. E.; Cross, J. B.; Bakken, V.; Adamo, C.; Jaramillo, J.; Gomperts, R.; Stratmann, R. E.; Yazyev, O.; Austin, A. J.; Cammi, R.; Pomelli, C.; Ochterski, J. W.; Martin, R. L.; Morokuma, K.; Zakrzewski, V. G.; Voth, G. A.; Salvador, P.; Dannenberg, J. J.; Dapprich, S.; Daniels, A. D.; Farkas; Foresman, J. B.; Ortiz, J. V.; Cioslowski, J.; Fox, D. J. . (2009) Gaussian 09, Gaussian, Inc., Wallingford, CT.
2. Anisimov, V. P., P. (1999) ISOEFF98: A program for studies of isotope effects using Hessian modifications. *J. Math Chem.* 26, 75–86.
3. Thomas, K., Cameron, S. A., Almo, S. C., Burgos, E. S., Gulab, S. A., and Schramm, V. L. (2015) Active site and remote contributions to catalysis in methylthioadenosine nucleosidases. *Biochemistry* 54, 2520–2529.
4. Fadoulglou, V. E., Kokkinidis, M., and Glykos, N. M. (2008) Determination of protein oligomerization state: two approaches based on glutaraldehyde crosslinking. *Anal. Biochem.* 373, 404–406.
5. Yuan, H., Stratton, C. F., Evans, G., Tyler, P., and Schramm, V. L. (2016) *submitted, ACS Chem. Biol.*
6. Parkin, D. W., Leung, H. B., and Schramm, V. L. (1984) Synthesis of nucleotides with specific radiolabels in ribose. Primary <sup>14</sup>C and secondary <sup>3</sup>H kinetic isotope effects on acid-catalyzed glycosidic bond hydrolysis of AMP, dAMP, and inosine. *J. Biol. Chem.* 259, 9411–9417.
7. Shafqat, N., Muniz, J. R., Pilka, E. S., Papagrigoriou, E., von Delft, F., Oppermann, U., and Yue, W. W. (2013) Insight into *S*-adenosylmethionine biosynthesis from the crystal structures of the human methionine adenosyltransferase catalytic and regulatory subunits. *Biochem. J.* 452, 27–36.
8. Singh, V., Lee, J. E., Nunez, S., Howell, P. L., and Schramm, V. L. (2005) Transition state structure of 5'-methylthioadenosine/*S*-adenosylhomocysteine nucleosidase from *Escherichia coli* and its similarity to transition state analogues. *Biochemistry* 44, 11647–11659.
9. Rose, I. A. (1980) The isotope trapping method: desorption rates of productive E.S complexes. *Methods Enzymol.* 64, 47–59.



10. Kim, S., Bolton, E. E., and Bryant, S. H. (2013) PubChem3D: conformer ensemble accuracy. *J. Cheminform.* 5, 1.
11. Lee, J. E., Cornell, K. A., Riscoe, M. K., and Howell, P. L. (2003) Structure of *Escherichia coli* 5'-methylthioadenosine/ S-adenosylhomocysteine nucleosidase inhibitor complexes provide insight into the conformational changes required for substrate binding and catalysis. *J. Biol. Chem.* 278, 8761–8770.
12. Copeland, R. A. (2000) *Enzymes*, Vol. Second Edition, Wiley, Canada.